INTERNATIONAL JOURNAL OF AGRICULTURE & BIOLOGY
ISSN Print: 1560–8530; ISSN Online: 1814–9596
09–273/YHP/2010/12–1–101–105
http://www.fspublishers.org

Full Length Article

Monitoring Development and Ripeness of Oil Palm Fruit (*Elaeis guneensis*) by MRI and Bulk NMR

SHARIFUDIN MD. SHAARANI[1]‡, ARTURO CÁRDENAS-BLANCO, M.H. GAO AMIN, N.G. SOON† AND LAURANCE D. HALL

Herchel Smith Laboratory for Medicinal Chemistry, University of Cambridge School of Clinical Medicine, University Forvie Site, Robinson Way, Cambridge, CB2 2PZ, UK

†*Department of Chemistry, Faculty of Science, University Malaya, 50603 Kuala Lumpur, Malaysia*

‡*School of Food Science and Nutrition, University Malaysia Sabah, Locked Bag 2073. Kota Kinabalu 88999, Sabah, Malaysia*

[1]Corresponding author's e-mail: fatihah@ums.edu.my

ABSTRACT

In this study, magnetic resonance imaging (MRI) and bulk nuclear magnetic resonance (NMR) were used to track the progressive development of intact oil palm fruit (variety Tenera). Fresh fruits were harvested at 4, 12, 16 and 21 weeks after anthesis (WAA) and all measurements of spin-spin relaxation times (T_2-values) were performed at 2.35 Tesla and 20ºC. MR imaging data were fitted to mono-exponential decay curves, which depicted a progressive increase in the mean T_2–values for mesocarp (18-32 ms) and kernel (13-74 ms) with WAA. The same data were also fitted to bi-exponential decay curves for both the mesocarp and kernel, which showed a decrease of the T_{21}-values from 12-10 ms and 10-9 ms, respectively and an increase of the T_{22}-values from 83-118 ms and 129-139 ms, respectively with WAA; those two components are assigned to the protons of water (T_{21}) and to those of the oil (T_{22}). The multi-exponential fitting of the bulk NMR T_2 relaxation data for the intact fruit demonstrated three distinct components; T_{21} (intermediate component, 23-30 ms) and T_{22} (long component; 64-144 ms), which are assigned to water protons and oil, respectively and T_{23} (short component; 3-6 ms) related to the shell. The bulk NMR T_2 relaxation data for the kernel also demonstrated three components; T_{21} (intermediate component, 12-22 ms) and T_{22} (long component, 59-135 ms), which was assigned to water bound in the endosperm (kernel) and oil content respectively, while short component T_{23} (3-2 ms) was associated to the shell.

Key Words: MRI; NMR; Oil palm fruit; Ripening

INTRODUCTION

Oil palm is the world's second largest vegetable oil source after soybean oil and contributes for 13% of the total world production of oils and fats (Sambanthamurthi *et al.*, 2000). It is nutritional for health and is a raw material for the oleo chemical industries. It is a major crop in Malaysia giving an annual average yield amounting to 4 t ha^{-1} annually (Sapak *et al*., 2008).

The oil palm fruit is a sessile drupe fruit and its pericarp consists of exocarp (skin), mesocarp (pulp) and endocarp (shell); for the investigated variety Tenera the shell is 0.5-4 mm thick. Fruits at the tip of each spikelet ripen first and those at the base last; those on the outside of the bunch are large and deep orange when ripe, while inner fruits are smaller and paler (Hartley, 1988).

The development of oil palm fruit starts about 2 weeks after anthesis (WAA); at 8 WAA the endosperm of the seed is liquid and at 10 WAA it is semi-gelatinous (Oo *et al.*, 1985; Hartley, 1998). At 12 WAA oil starts to deposit in the endosperm and almost complete by 16 WAA. During this period the endosperm and endocarp slowly harden and by 16 WAA the endocarp is a hard shell enclosing a hard, whitish endosperm, which is known as the kernel (Oo *et al*., 1985; Sambanthamurthi *et al*., 2000). Oil deposition in the mesocarp starts at about 15 WAA and continues until fruit maturity (about 20 WAA) (Bafor & Osagie, 1986; Sambanthamurthi *et al*., 2000). According to Oo *et al.* (1985), as the total lipid progressively increases (0.1 - 48%) in the mesocarp the moisture content decreases (88-37%) with WAA. It is important to understand the biochemical, morphological and physiological process during ripening process, which can help to improve the characteristic of a fruit (Al-Maaitah *et al.*, 2009).

The conventional way to determine the ripening of oil palm fruit is by counting the number of fruits loose per bunch (Hartley, 1998). After harvesting the fruit are graded manually according to their color, which establishes the grade and quality of the extracted oil. Recently Abdullah *et al.* (2004) studied the use of automated machine vision to

To cite this paper: Shaarani, S.Md, A. Cárdenas-Blanco, M.H.G. Amin, N.G. Soon and L.D. Hall, 2010. Monitoring development and ripeness of oil palm fruit (*Elaeis guneensis*) by MRI and bulk NMR. *Int. J. Agric. Biol.*, 12: 101–105

grade oil palm fruit. There were several studies to measure the progressive changes of oil content in the oil palm fruit mesocarp (Oo *et al*., 1986; George & Arumughan, 1991; George & Arumughan, 1993; Bafor & Osagie, 1998) and also measured the decrease in moisture content during ripening (Khalid & Hua, 1998; Abdullah *et al*., 2004).

It is already known (McCarthy, 1994; Hills, 1998) that measurements of the Magnetic Resonance (MR) properties of the protons of water or lipid in food materials can provide valuable information about the physical and chemical properties of food, which can be made non-destructively and non-invasively. Although Magnetic Resonance Imaging (MRI) has not yet been widely used industrially, nevertheless it is clearly recognized that MRI can characterized the quality of various food such as texture (Barreiro *et al*., 2000; Nott *et al.,* 2003), Moisture content (Ishida *et al.,* 2004; Md Shaarani *et al.,* 2006) and pH (Evans & Hall, 2005), provide insight to its processing such as freezing (Evans *et al.,* 1999), heating (Md Shaarani *et al.,* 2005), storage (Miquel & Hall, 2002), ripening (Létal *et al.,* 2003; Galed *et al.,* 2004) and postharvest studies of fruits and vegetables (Clark *et al.,* 1997; Kim *et al.,* 1999).

In this study both MRI and bulk NMR techniques are employed to monitor the development of oil palm fruit and to follow the ripening process by measuring the progressive changes in the spin-spin relaxation times (T_2-values) of the protons of the water and lipid.

MATERIALS AND METHODS

Sample preparation: The oil palm fruits (*Elaeis guneensis*, variety *Tenera*) were collected from the Malaysian Palm Oil Board [MPOB, formerly known as Palm Oil Research Institute of Malaysia (PORIM)] experimental station. Fresh fruit bunches were harvested at specific stages (4, 12, 16 & 21 WAA) of maturity and spikelets of fruits were separated from bunches. A total of eight intact *Tenera* variety oil palm fruits (two from each WAA) were separated from the spikelets, cleaned and dried.

MRI and Bulk NMR T_2 measurements: All MRI measurements were made using a Bruker Medzintechnik Biospec II imaging console (Karlsruhe, Germany) connected to a 2.35 Tesla, 31 cm horizontal-bore superconducting magnet (Oxford Instruments, Oxford, U.K). Each axis of the gradient set (11.6 cm internal diameter) was powered by a pair of Tecron gradient amplifiers (Model 7790, Crown International Inc., Elkart, IN, U.S.A). A cylindrical, eight-strut, bird-cage radiofrequency (RF) probe (internal diameter 5.9 cm) was used in quadrature mode to transmit and receive the MR signals.

MRI quantification of the spin-spin (T_2) relaxation times and corresponding liquid proton densities (M_0) were acquired using a multi echo Carr-Purcell-Meiboom-Gill (CPMG) pulse sequence (Boulby & Rugg-Gunn, 2003) for 2D slice images (313 x 313 µm in-plane resolution, 3 mm slice thickness, 4 averages) and performed at 20ºC. A set of 32 multi-echo images were acquired with the echo time (TE) 6 ms and TR 2.0 s, scan time 18 min. During imaging, a reference sample of 100% crude palm olein oil was located by the side of each sample within the imaging field of view.The resultant sets of T_2-multi-echo images were fitted to a mono-exponential decay model for T_2 given by Equation 1:

$$M_{xy}(t) = M_0 e^{(-t/T2)} \quad (1)$$

Where $M_{xy}(t)$ is the magnetization at the echo time 't' of each echo in a particular pixel, M_0 is the equilibrium magnetization (proportional to the liquid proton density), T_2 is the transverse relaxation time. Least squares fitting of signals in each pixel to a mono-exponential T_2 relaxation decay model gave the spatial distribution of T_2-values. The corresponding M_0-values were obtained by extrapolating each pixel of the fitted transverse decay back to zero time. The data analyses used a curve fitting program written-in-house by Dr P. Watson, which based on the method of Levenberg-Marquandt (Marquardt, 1963).

The same sets of data were also processed using a bi-exponential fitting algorithm written in Matlab (Mathworks, Natwick, MA), which calculated the M_0 and T_2–values for the two main components (water & oil) of the oil palm nut. The T_2 multi-echo images were fitted to the corresponding bi-exponential decay curves given by Equation 2:

$$M_{xy}(t) = M_{01}\,EXP\,(-t/T_{21}) + M_{02}\,EXP\,(-/tT_{22}) \quad (2)$$

Bi-exponential fitting requires more number of echoes and a good signal-to-noise ratio; (Henkelman, 1985; Anastasiou & Hall, 2004). As a result this will increase the scanning time.

The bulk NMR T_2 measurements were acquired using a Carr-Purcell-Meiboom-Gill (CPMG) sequence with 256 echoes, TE 1.0 ms and TR 10 seconds. The experimental data were fitted to the tri-exponential decay curves using Equation 3, with the aid of Levenberg-Marquandt (Marquardt, 1963) least-squares optimization method (Gnuplot software, Linux version 3.7):

$$M_{xy}(t) = M_{01}\,EXP(-t/T_{21}) + M_{02}\,EXP(-t/T_{22}) + M_{03}\,EXP(-t/T_{23}) \quad (3)$$

RESULTS AND DISCUSSION

Fruit morphology: The MR images in (Fig. 1a & b) clearly show the different parts of an oil palm fruit aged 4 WAA. At this stage, hardly <1% oil deposits in the mesocarp and most of the MR signal come from the protons of the water (85-88%) in the fruit (Oo *et al.,* 1985; Bafor & Osagie, 1986). The black region in the middle corresponds to the empty shell, because the kernel (a solid, whitish endosperm) is not yet developed. At 21 WAA (Fig. 1c & d), the fruit matures and ripens and the moisture content has decreased to 30%, due to the oil accumulation in the mesocarp to 60% (Oo *et al.,* 1985; Bafor & Osagie, 1986). Thus the MR signals come from the protons of oil rather than water protons and the high intensity regions have higher concentrations of oil.

Fig. 1: The 2D images of oil palm fruit 4 weeks after anthesis in (a) the axial orientation with spatial resolution of 117 x 117 µm, (b) sagittal orientation (193 x 121 µm), At 21 weeks after anthesis (c) shows the sagittal orientation (193 x 121 µm) and (d) the axial orientation (133 x 125 µm), All data were measured at 4.7 Tesla; TE/TR/Slice thickness: 10.4 ms/2000 ms/1.5 mm; Matrix = 256 x 256; 4 averages; Scan time = 34 minutes

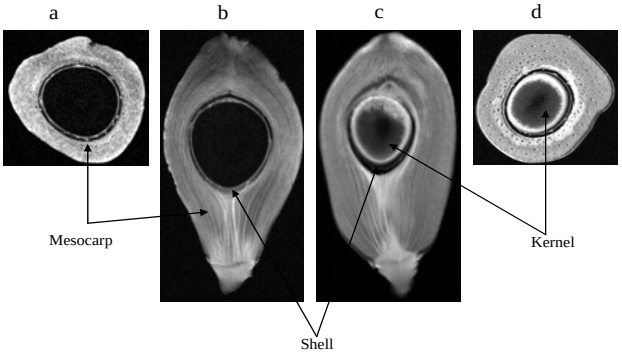

Fig. 2: The distribution of the T_2 values for (a) mesocarp and (b) kernel at 4, 12, 16 and 21 weeks after anthesis, the corresponding mean T_2 values for the mesocarp and kernel for those same fruit are given in c and d

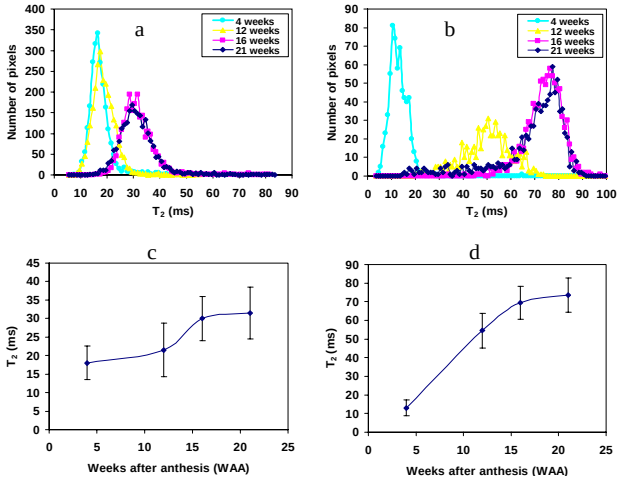

T_2 Measurements from MR Imaging

Mono-exponential fitting: Fig. 2a and b are histogram plots of the distributions of the T_2-values for the mesocarp and kernel of oil palm fruit, while the mean and standard deviation of those T_2 measurements with WAA are illustrated in (Fig. 2c & d) respectively. The T_2 distributions for the mesocarp at both 4 and 12 WAA are narrow, because the main component is water; however at 16 and 20 WAA the distribution is broader, because of the increasing accumulation of oil. The mean T_2–values for the mesocarp at 4, 12, 16 and 20 WAA are 18 ± 5 ms, 22 ± 7 ms, 30 ± 6 ms and 32 ± 7 ms, respectively (Fig. 2c). The progressive increase in those values suggests that there are fewer bound and more free, protons in the mesocarp, which is certainly consistent with increased oil content. The T_2-values for the kernel at 4 WAA have a narrower distribution compared to the other stages of WAA; at 12 and 16 WAA the distribution gets progressively broader, which indicates the increasing oil deposition in the kernel. The mean T_2–values at 4, 12, 16 and 20 WAA are 13 ± 4 ms, 55 ± 9 ms, 70 ± 8 ms and 74 ± 5 ms (Fig. 2d) and that progression also reflects the increasing of the oil content in the kernel.

Bi-exponential fitting: Bi-exponential fitting of T_2–relaxation data enabled separation of two individual structural components according to their spin-spin relaxation times (T_2–values). The distribution of T_{21}–values (Fig. 3a) for the mesocarp showed a decrease (12-10 ms), whereas the T_{22}–values (Fig. 3b) increased (83-108 ms) with WAA. Based on the known fact (Oo *et al*., 1985; Bafor & Osagie, 1986; Sambanthamurthi *et al.*, 2000) that while the moisture content decreases, the oil content increases with WAA, it can be inferred that T_{21} is related to the protons of water and T_{22} to those of oil. The same phenomenon is observed for the kernels; thus the distribution of T_{21} (Fig. 3c) decreased (10-9 ms), while T_{22} (Fig. 3d) increased (127-139 ms) with WAA; the 4 WAA, T_2 distribution is excluded from this analyses since its main component is water. The trend showed by T_{21} and T_{22} for both of the mesocarp and kernel is parallel to the data in the literature (Oo *et al*., 1985; Bafor & Osagie, 1986; Khalid & Abbas, 1992; Sambanthamurthi *et al.*, 2000) based on measurements of moisture and oil content.

Normalised M_0 from T_2 measurements: Fig. 4a and b are the M_{02} maps of the oil content in the oil palm fruit for 12 and 21 WAA, respectively. It is interesting to note the high oil content around the outer part of the kernel at 12 WAA (Fig. 4a), which suggests, that for this sample the development of the oil in the kernel starts from the outside and then continues to deposit at the centre. By 21 WAA, the oil content is more evenly distributed in both the mesocarp and the kernel (Fig. 4b).

The normalised M_{02} values (M_0 sample/M_0 reference) for the mesocarp (Fig. 4c) show an increase from 12 to 16 and 21 WAA, which illustrates the consistency of the MRI measurements with the literature (Oo *et al*., 1985; Bafor & Osagie, 1986; George & Arumughan, 1991) and reports that the gravimetric oil content increases with WAA. The kernel (Fig. 4d) also showed an increase from 12 to 16 WAA; although there is a small decrease in peak from 16 to 21 WAA, but the total area under curve for 21 WAA is higher than 16 WAA. This indicates there was an increase in the oil content from 16 to 21 WAA as reported by other researchers (Oo *et al*., 1986; Bafor & Osagie, 1986; George & Arumughan, 1991).

Fig. 3: The T_{21} and T_{22} distributions obtained by bi-exponential fitting for the mesocarp (a, b) and kernel (c, d) at 12, 16 and 21 weeks after anthesis (WAA)

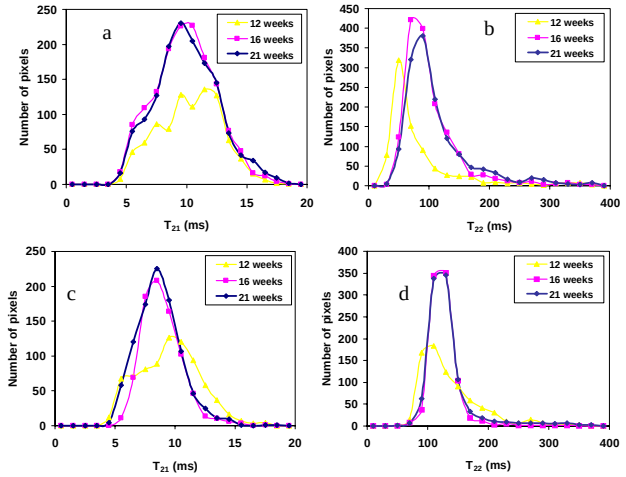

Fig. 4: The M_{02} map for an intact oil palm fruit measured at 12 WAA (a) and 21 WAA (b). the M_{02} distribution for the mesocarp (c) and kernel (d) calculated by bi-exponential fitting data for fruit at 12, 16 and 21 weeks after anthesis (WAA)

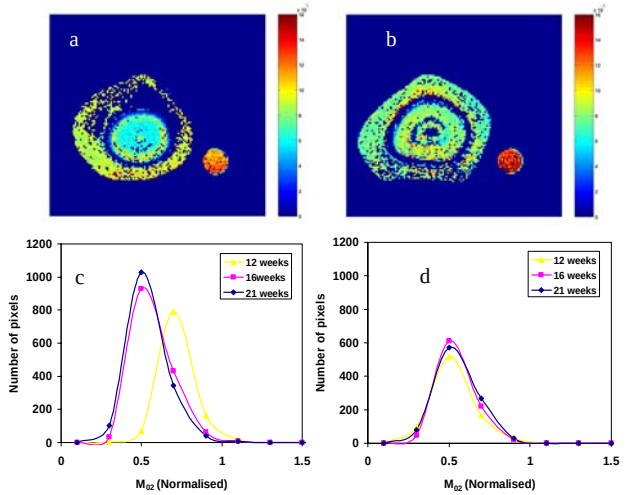

Bulk NMR T_2 Measurements

Intact fruit: Multi-exponential fitting of the bulk NMR T_2 relaxation data from intact fruits identified three distinct components: a long component (T_{22}) of 64-144 ms, an intermediate component (T_{21}) of 23-30 ms (Fig. 5a & b) and a short component (T_{23}) 3-6 ms. It is suggested that the long component (T_{22}) is related to the oil content since it increases substantially with WAA. The intermediate component (T_{21}) represents water bound in the mesocarp and kernel tissues, whereas the short component (T_{23}) is assigned to the protons bounded in the shell.

Kernel. In order to make specific measurements of the kernel the oil palm fruit was cut open. Analysis of the T_2 data from those isolated kernels also demonstrated three

Fig. 5: The T_2 and M_0 values calculated from bulk NMR measurements of intact oil palm fruit (a, b) and the kernel (c, d), at 4, 12, 16 and 21 weeks after anthesis (WAA)

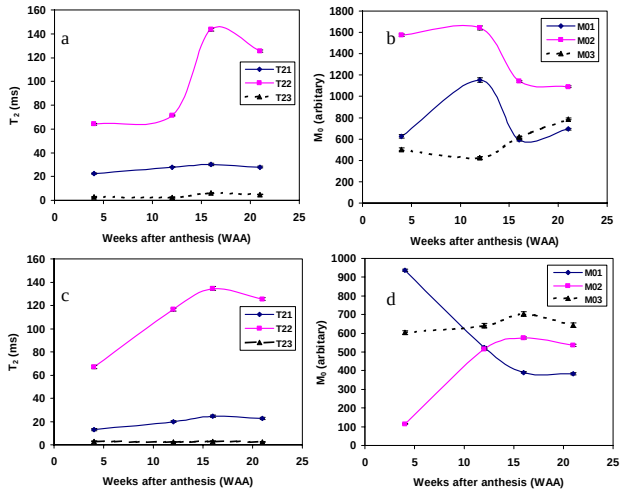

distinct components (Fig. 5c & d): a long component T_{22} = 59-135 ms, an intermediate major component T_{21} = 12-22 ms and short component T_{23} = 3-2 ms. Again it is suggested that the long component is related to the oil content, the intermediate component (T_{21}) represents water bound in the endosperm (kernel) and the short component (T_{23}), is assigned to water associated with the shell.

CONCLUSION

This study has demonstrated that both MRI and bulk NMR effective techniques to measure the ripening of an intact oil palm fruit. The mono-exponential and bi-exponential curve fit to T_2 data obtained from MRI provided reliable information about the oil and moisture content, which was separately measured, because of the difference in their spin-spin relaxation time. The increase in T_2 values for both mesocarp and kernel with WAA indicated the increase in the oil content in both components of the fruit. The multi-exponential fitting of the bulk NMR T_2 relaxation data for the intact fruit demonstrated three distinct components; T_{21} (intermediate component, 23-30 ms) represents the water and T_{22} (long component; 64-144 ms) assigned to oil, while T_{23} (short component; 3-6 ms) was related to the shell.

Acknowledgement: It is a pleasure to thank the following for their support: the late Dr Herchel Smith for his endowment to the late LDH. Thanks are also due to Richard Smith, Simon Smith and Cyril Harbird for supply and maintenance of the MRI hardware; Dr Da Xing and Dr Nicholas Herrod for the computer facilities and software, respectively and Dr Paul Watson for the curve fitting software. We also thank Dr. Ravigadevi Sambanthamurthi of the Malaysian Palm Oil Board for providing the oil palm fruits and arranging the tagging of the fruit inflorescences in the experimental station.

REFERENCES

Abdullah, M.Z., L.C. Guan, K.C Lim and A.A. Karim, 2004. The application of computer vision system and tomographic radar imaging for assessing physical properties of food. *J. Food Eng.*, 61: 125–135

Al-Maaitah, M.I., K.M. Al-Absi and A. Al-Rawashdeh, 2009. Oil quality and quantity of three olive ciltivars as influenced by harvesting date in the middle and southern parts of Jordan. *Int. J. Agric. Biol*., 11: 266–272

Anastasiou, A. and L.D. Hall, 2004. Optimization of T_2 and M_0 measurements of bi-exponential systems. *Magn. Reson. Imaging*, 22: 67–80

Bafor, M.E. and A.U. Osagie, 1986. Changes in lipid class and fatty acid composition during maturation of mesocarp of oil palm (*Elaeis guineensis*) variety Dura. *J. Sci. Food Agric.*, 37: 825–832

Bafor, M.E. and A.U. Osagie, 1998. Changes in non-polar lipid composition of developing oil palm fruit (*Elaeis guineensis*) mesocarp. *J. Sci. Food Agric.*, 45: 325–331

Barreiro, B., C. Ortiz, M. Ruiz-Altisent, J. Ruiz-Cabello, M.E. Fernández-Valle, I. Recasens and M. Asensio, 2000. Mealiness assessment in apples and peaches using MRI techniques. *Magn. Reson. Imaging*, 18: 1175–1181

Clark, C.J., L.N. Drummond and J.S. MacFall, 1998. Quantitative magnetic resonance imaging of kiwi-fruit during growth and ripening. *J. Sci. Food Agric.*, 78: 349–358

Clark, C.J., P.D. Hockings, D.C. Joyce and R.A. Mazucco, 1997. Application of magnetic resonance imaging to pre-and post harvest studies of fruits and vegetables. *Postharvest Biol. Technol*., 11: 1–21

Evans, S.D., K.P. Nott and L.D. Hall, 1999. Quantitative magnetic resonance imaging on fresh and frozen-thawed trout. *Magn. Reson. Imaging.*, 17: 445–455

Evans, S. and L.D. Hall, 2005. Measurements of pH in food systems by magnetic resonance imaging. *Canadian J. Chem. Eng.*, 83: 73–77

Galed, G., M.E. Fernández-Valle, A. Martinez and A. Heras, 2004. Application of MRI to monitor the process of ripening and decay in citrus treated with chitosan solutions. *Magn. Reson. Imaging*, 22: 127–137

George, S. and C. Arumughan, 1991. Distribution of lipids on the exocarp and mesocarp of three varieties of oil palm fruit (*Elaeis guineensis*). *J. Sci. Food Agric.*, 56: 219–222

George, S. and C. Arumughan, 1993. Positional distribution of fatty acids in the triacylglycerols of developing oil palm fruit. *J. American Oils Chem. Soc.*, 70: 1255–1258

Hartley, C.W.S., 1988. *The Oil Palm (Elaeis guineensis Jacq.)*, 3rd edition, pp: 207–210. Harlow: Longman Scientific and Technical Company

Henkelman, R.M., 1985. Measurement of signal intensities in the presence of noise in MR images. *Med. Phys.*, 12: 232–233

Hills, B., 1998. *Magnetic Resonance in Food Science*, pp: 76–101. New York US: John Wiley and Sons, Inc

Ishida, N., S. Naito and H. Kano, 2004. Loss of moisture from harvested rice seeds on MRI. *Magn. Reson. Imaging*, 22: 871–875

Khalid, K. and T.L. Hua, 1998. Development of conductor-backed coplanar waveguide moisture sensor for oil palm fruit. *Measuring Sci. Technol.*, 9: 1191–1195

Khalid, K.B. and Z. Abbas, 1992. A microstrip sensor for determination of harvesting time for oil palm fruits (Tenera: *Elaeis guineensis*). *J. Microwave Power Electromagn. Ener*., 27: 3–10

Kim, S.M., P. Chen, M.J. McCarthy and B. Zion, 1999 Fruit internal quality evaluation using on-line nuclear magnetic resonance sensors. *J. Agric. Eng. Res.*, 74: 293–301

Létal, J., D. Jirák, L. Šuderlová and M. Hájek, 2003. MRI texture analysis of MR images of apples during ripening and storage. *Lebensm-Wiss. U-Technol.*, 36: 719–727

Marquardt, D.W., 1963. An algorithm for least-squares estimation for non-linear parameters. *J. Soc. Indus. Appl. Math.*, 11: 431–441

McCarthy, M.J., 1994. *Magnetic Resonance Imaging in Foods*, pp: 70–80. New York US: Chapman and Hall, USA

Md Shaarani, S., K.P. Nott and L.D. Hall, 2005. Magnetic resonance measurements of structural changes during heating of chicken meat by hot air. *In*: Engelsen, S.B., P.S. Belton and H.J. Jakobsen (eds.), *Magnetic Resonance in Food: The Multivariate Challenge*, pp: 65–71. London: The Royal Society of Chemistry, UK

Md Shaarani, S., K.P. Nott and L.D. Hall, 2006. Combination of NMR and MRI quantitation of moisture and structure changes for convection cooking of fresh chicken meat. *Meat Sci*., 72: 398–403

Miquel, M.E. and L.D. Hall, 2002. Measurements by MRI of storage changes in commercial chocolate confectionary products. *Food Res. Int.*, 35: 993–998

Nott, K.P., S. Md Shaarani and L.D. Hall, 2003. The effect of microwave heating on potato texture as studied with magnetic resonance imaging. *In*: Belton, P.S., A.M. Gil and D. Rutledge (eds.), *Magnetic Resonance Food Science Latest Development*, pp: 38–45. The Royal Society of Chemistry, London

Nott, K.P. and L.D. Hall, 2004. New techniques for measuring and validating thermal process. *In*: Richardson, P. (ed.), *Improving the Thermal Processing of Foods*, pp: 385–407. Cambridge UK: Woodhead Publishing Limited, London

Oo, K.C., S.K. Teh, H.T. Khor and S.H.O. Augustine, 1985. Fatty acid synthesis in the oil palm (*Elaeis guineensis*): incorporation of acetate by tissue slices of the developing fruits. *Lipids*, 20: 205–209

Oo, K.C., K.B. Lee and S.H.O. Augustine, 1986. Changes in fatty acid composition of the lipid classes in developing oil palm mesocarp. *Phytochem.*, 25: 405–407

Sambanthamurthi, R., K. Sundram and Y. Tan, 2000. Chemistry and biochemistry of palm oil. *Prog. Lipid Res.*, 39: 507–558

Sapak, Z., S. Meon and Z.A. Mior Ahmad, 2008. Effect of endophtic on growth and suppression of *Ganoderma* infection in oil palm. *Int. J. Agric. Biol*., 10: 127–132

(Received 10 August 2009; Accepted 18 September 2009)